Phosphate ion channels in sarcoplasmic reticulum of rabbit skeletal muscle

Derek R. Laver, Gerlinde K. E. Lenz and Angela F. Dulhunty*

*School of Biochemistry and Molecular Biology, Faculty of Science, Australian National University, Canberra, ACT 0200, Australia and * John Curtin School of Medical Research, Australian National University, Canberra, ACT 0200, Australia*

(Resubmitted 8 February 2001; accepted after revision 24 May 2001)

1. Phosphate ions (P_i) enter intracellular Ca^{2+} stores and precipitate Ca^{2+}. Since transport pathways for P_i across the membrane of intracellular calcium stores have not been identified and anion channels could provide such a pathway, we have examined the P_i conductance of single anion channels from the sarcoplasmic reticulum (SR) of rabbit skeletal muscle using the lipid bilayer technique.

2. Two anion channels in skeletal muscle SR, the small conductance (SCl) and big conductance (BCl) chloride channels, were both found to have a P_i conductance of 10 pS in 50 mM P_i. The SCl channel is a divalent anion channel which can pass HPO_4^{2-} as well as SO_4^{2-} (60 pS in 100 mM free SO_4^{2-}). The BCl channel is primarily a monovalent anion channel. The SCl and BCl channels are permeable to a number of small monovalent anions, showing minor selectivity between Cl^-, I^- and Br^- ($Cl^- > I^- > Br^-$) and relative impermeability to cations and large polyatomic anions (Cs^+, Na^+, choline$^+$, Tris$^+$, Hepes$^-$ and $CH_3O_3S^-$).

3. The P_i conductance of SCl and BCl channels suggests that both channel types could sustain the observed P_i fluxes across the SR membrane. Comparison of the blocking effects of the phosphonocarboxylic acids, ATP and DIDS, on the anion channels with their effects on P_i transport suggests that the SCl channel is the more likely candidate for the SR P_i transport mechanism.

4. The SCl channel, with previously unknown function, provides a regulated pathway for P_i across the SR membrane which would promote P_i entry and thereby changes in the rapidly releasable Ca^{2+} store during onset and recovery from muscle fatigue. Anion channels may provide a pathway for P_i movement into and out of Ca^{2+} stores in general.

Phosphate ions (P_i, i.e. HPO_4^{2-} and $H_2PO_4^-$, see Methods) regulate the size of the rapidly releasable intracellular calcium pool, and hence physiological function, in a wide variety of cell types (Fulceri *et al.* 1993; Fryer *et al.* 1995; Guse *et al.* 1996; Mezna & Michelangeli, 1998). P_i is produced in the cytoplasm as a by-product of ATP metabolism. In resting muscle cytoplasmic [P_i] is in the range 1–5 mM, but during muscle fatigue [P_i] can rise to 20–40 mM (Godt & Nosek, 1989). At these levels P_i causes a marked reduction in Ca^{2+} release and peak muscle force (Fryer *et al.* 1995; Kabbara & Allen, 1999). Three mechanisms for this have been proposed. Firstly, depletion of the ryanodine-sensitive Ca^{2+} stores by activation of the calcium release channels. Bilayer studies indicate that cytoplasmic P_i can activate the calcium release channels in the sarcoplasmic reticulum (SR) (Fruen *et al.* 1994). Secondly, depletion of Ca^{2+} by reversal of the Ca^{2+}-ATPase. High cytosolic [P_i], in conjunction with low creatine phosphate levels, is believed to reverse the SR Ca^{2+}-ATPase in skinned muscle fibres (Duke & Steele, 2000). Finally, reduction of the free [Ca^{2+}] in stores when P_i enters the lumen of InsP_3- and ryanodine-sensitive Ca^{2+} stores and forms a variety of insoluble Ca^{2+}–P_i precipitates (Fulceri *et al.* 1993; Fryer *et al.* 1995; Fryer *et al.* 1997). Although these effects of P_i transport across the SR can be dramatic, P_i pathways between cytoplasm and lumen have not been identified. Stefanova *et al.* (1991*a*) observed ATP-dependent transport of P_i across the membrane of SR vesicles. The fact that ATP enhanced this transport suggested an active mechanism. However, recent studies by Posterino & Fryer (1998) in skinned muscle fibres have suggested that P_i entry and exit from the SR primarily occur through a passive pathway that is not driven by ATP. In fact, these authors found that P_i entry into the SR was *facilitated* when ATP was omitted from the myoplasmic solution, a result consistent with P_i entry through an ATP-inhibited anion channel. However, there are no reports of P_i-permeable channels in the SR membrane.

Two SR anion channels have been identified in rabbit skeletal muscle. The BCl channel (250 pS in 250/50 mM

Cl^-; *cis/trans*) is apparently unregulated by cytoplasmic ligands and is constitutively open in lipid bilayers (Tanifuji *et al.* 1987; Kourie *et al.* 1996*b*). The smaller conductance SCl channel (75 pS in 250/50 mM Cl^-) is highly regulated, and partially inhibited by cytoplasmic acidification (< pH7), millimolar concentrations of adenine nucleotides (Ahern & Laver, 1998; Kourie, 1999) and inositol phosphates (Kourie *et al.* 1997). It is voltage dependent (open at membrane potentials, V_m, between 0 and −80 mV with respect to the luminal side, Kourie *et al.* 1996*b*), activated and inhibited by oxidation and reduction, respectively (Kourie, 1997*a*) and activated by ~1 μM cytoplasmic Ca^{2+} (Kourie *et al.* 1996*a*).

In muscle there appears to be an excess of SR Cl^- channels even though Cl^- is not an important counterion during Ca^{2+} release from SR (Coonan & Lamb, 1998). The presence of the anion channels could be understood if intracellular Cl^- channels also conducted physiologically important anions other than Cl^-. Thus we have measured the conductance of SCl and BCl channels to inorganic phosphate to determine whether the channels could play a role in passing these functionally important anions.

METHODS

Isolation and reconstitution SR anion channels

SR vesicles were prepared from the back and leg muscle of New Zealand White rabbits as described by Saito *et al.* (1984). Rabbits (~4 kg) were killed by captive bolt before muscle was removed for biochemical processing. The procedure was carried out by the holder of a current licence granted under ACT State legislation by the Australian National University Ethics Committee. SR vesicles were isolated from muscle using techniques based on Chu *et al.* (1988) as previously described in Laver *et al.* (1995) and Kourie *et al.* (1996*b*). Briefly, cubes of muscle were homogenized in a Waring blender in homogenizing buffer (20 mM imidazole, 300 mM sucrose, pH 7.1 with HCl), centrifuged (11 000 *g*, 15 min) and the pellet resuspended, rehomogenized and centrifuged as above. The supernatant was filtered through cotton gauze and pelleted by centrifugation (110 000 *g* for 60 min) to yield a crude microsomal fraction, which was fractionated by loading onto a discontinuous sucrose gradient. Heavy SR vesicles were collected from the 35–45% (w/v) interface, snap frozen and stored at −70 °C. SR vesicles were incorporated into artificial bilayers separating *cis* and *trans* baths. Details of the method are given elsewhere (Kourie *et al.* 1996*a*,*b*). Vesicles were added to the *cis* bath and the cytoplasmic side of incorporated channels faced the *cis* solution. The luminal side faced the *trans* solution.

Chemicals and solutions

Phosphoric acid was obtained from BDH and CsOH from ICN Biomedicals. 4′4′-Diisothiocyanatostilbene-2′2′-di-sulfonic acid (DIDS) was obtained from ICN Biomedicals. Phosphonoformic acid (PFA) and phenylphosphonic acid (PhPA) were obtained from Sigma. Lipids were obtained from Avanti Polar Lipids (Alabaster, AL, USA). Lipid bilayers were formed from phosphatidylethanolamine and phosphatidylcholine (8:2 w/w) in *n*-decane, across an aperture of 150–250 μm diameter in a Delrin cup.

Unless otherwise stated, solutions were buffered to pH 7.4 using 10 mM TES and also contained 0 (no added Ca^{2+}) to 1 mM $CaCl_2$ (Kourie *et al.* 1996*b*). The current through SCl and BCl channels was investigated in the presence of P_i solutions with Na^+, Cs^+ or $Tris^+$ as the cation. Na_xP_i-containing solutions were made by mixing Na_2HPO_4 and NaH_2PO_4 solutions in a ratio of 81:19, titrating one with the other to give a final pH of 7.4. $Tris_xPi$ and Cs_xP_i solutions were produced by titrating phosphoric acid with Tris-base and CsOH, respectively, to the desired pH. TES was not required to buffer the pH of P_i solutions. The relative permeability of P_i was mainly determined with 50–200 mM P_i on one side of the membrane and either 250 mM CsCl or choline-Cl on the other. Concentrations given for P_i solutions refer to P_i, not the cation.

Sulphate-containing solutions were either $MgSO_4$ or Cs_2SO_4. Sulphate permeability was measured with 50–250 mM SO_4^{2-} on one side of the membrane and 250 mM of either CsCl or choline-Cl on the other. The free [SO_4^{2-}] was estimated using published association constants (Marks & Maxfield, 1991) and the program 'Bound and Determined' (Brooks and Storey, 1992). Measurement of channel permeability to Br^- and I^- (Y) relative to Cl^- was made using 250 mM CsCl or choline-Cl on one side of the bilayer and 250 mM CsY (occasionally 50 mM CsY) on the other.

Individual ion channels were usually studied under several different ionic conditions during each experiment. Channels were initially identified as BCl or SCl by their conductance and gating properties in solutions containing 250/50 mM Cl^- (*cis/trans*). Ionic composition of the baths was then altered using three methods. (1) Bath solution exchange by perfusion with 10 volumes of solution using a back-to-back syringe system. (2) Aliquot addition of concentrated stock solutions to the baths. (3) Rapid local perfusion achieved by flowing solutions from a tube (polyethylene, 0.5 mm diameter, 50 μm from bilayer) directly onto the bilayer surface. At a flow rate of ~1 μl s^{-1}, the solution at the bilayer surface could be completely replaced with the perfusing solution in less than 1 s and the changed environment could be maintained for many minutes. Details of this technique are given elsewhere (Laver & Curtis, 1996).

Calculation of liquid junction and membrane potentials

Current was measured via agar-bridge electrodes (250 mM CsCl in 1% agar) in each solution. Bilayer potential is given with respect to the *trans* (luminal) bath and positive current signifies movement of positive charge from *cis* to *trans* solutions. Voltage was controlled and current recorded with an Axopatch 200B amplifier (Axon Instruments). The bilayer potential was calculated from the amplifier command potential and the liquid junction potentials at the agar electrode–bath interfaces, the *cis–trans* bath interface and the interface between locally perfused solutions and bath solution. In the case of solutions mainly containing monovalent ions, the liquid junction potentials can be calculated using the Henderson equation (eqn (1), e.g. Barry & Lynch, 1991).

$$E^S - E^P = (RT/F)S_F \ln\left(\sum_{i=1}^{N} z_i^2 u_i a_i^P \Big/ \sum_{i=1}^{N} z_i^2 u_i a_i^S\right), \quad (1)$$

where

$$S_F = \sum_{i=1}^{N}[(z_i u_i)(a_i^S - a_i^P)] \Big/ \sum_{i=1}^{N}[(z_i^2 u_i)(a_i^S - a_i^P)],$$

where E^P and E^S are the electric potentials in solutions *P* and *S* respectively and z_i, u_i and a_i are the valency, mobility and activity of ion species i, respectively. The Henderson equation does not accurately predict liquid junction potentials for solutions containing divalent ions. Liquid junction potentials were measured at the interface of dissimilar solutions in the *cis* and *trans* baths of the bilayer apparatus. The potential difference was measured relative to that obtained when *cis* and *trans* baths contained identical solutions (i.e. when the liquid junction potential equals zero). The potential difference between the two baths, at zero current, was measured using agar-bridge electrodes containing 4 M KCl while stirring the baths. We found that for electrolytes containing the monovalent ions used in this study, the Henderson equation predicted junction

potentials within ± 2 mV of those found experimentally, but this was not always the case for solutions containing divalent ions. Hence, we frequently used the Henderson equation to predict liquid junction potentials in the absence of divalent ions. We also measured changes in the liquid junction potentials at the agar electrode–bath interface that would occur during bath perfusion and we found that they were within 2 mV of those measured in free solutions. This was done by measuring the potential difference, at zero current, between an agar electrode containing 250 mM CsCl and one containing 4 M KCl both before and after the bath solution was changed.

Recording and analysis of single channel data

During the experiments the bilayer current and potential were recorded at a bandwidth of 5 kHz, sampled at 50 kHz and simultaneously stored on computer disk using a data interface (Data Translation DT301) with in-house software written in Visual Basic. Unitary current and time-averaged currents were extracted using Channel2 software (Professor P. W. Gage & Mr M. Smith at the Australian National University).

SCl channel unitary current was measured from the difference between the channel open and baseline (closed) current levels obtained at 23 ± 2 °C. Since the BCl channels rarely showed complete closures (see Results) it was difficult to directly measure the baseline current. For BCl channels the baseline current was determined in one of two ways, (1) from the mean current at the reversal potential of the BCl channel (V_r was found by adjusting the voltage to minimise the current variance) or (2) from occasional apparent closures of the channel. Channels in 'leaky' bilayers, in which significant baseline conductance was present (> 100 pS), were excluded from subsequent analysis. The conductance (G) of channels was determined from the slope of their current–voltage dependence. Relative ion permeability (P_j) was derived from the reversal potentials (V_r, where the current, I, is zero) for each set of ionic conditions by numerically solving the constant field equation (eqn (2)) (Goldman 1943):

$$I = 0 = \sum_j \left(\frac{V_r z_j^2 F}{RT}\right) P_j \left(\frac{a_{jcis} - a_{jtrans} e^{V_r z_j F/RT}}{1 - e^{V_r z_j F/RT}}\right), \quad (2)$$

where j are the ion species present, each with activity α_j and valency, z_j and V, F, R and T have their usual meanings. In calculating ionic permeabilities from the current reversal potentials it was assumed that cations and large anions (i.e. Cs^+, Na^+, choline$^+$, Tris$^+$, Hepes$^-$ and $CH_3O_3S^-$) had zero permeability. This assumption was supported by other measurements of V_r (shown for Cs^+ and choline$^+$ in Fig. 1), which indicated that the permeability of cations and large anions, relative to Cl^- was less than 0.05 in SCl and BCl channels. We found that the calculated permeability ratios for the smaller anions were insensitive to the assumed relative permeability values for cations and large anions over the range 0–0.05.

Ion activity coefficients, γ_j, for each species were calculated from the total ionic strength, μ, using the Guy-Chapman 'Limiting Law' (eqn (3)) which provides a good approximation to the experimentally observed mean activity coefficients at ionic strengths below 1 M (Margolis, 1966):

$$-\log\gamma_j = 0.509 z_j^2 \sqrt{\mu}/(1 + \sqrt{\mu}). \quad (3)$$

The Michaelis-Menten constants were determined by fitting eqn (4) (by the method of least squares) to the substrate concentration dependence of channel conductance. Fitting was carried out using results from individual experiments rather than the averaged data presented here:

$$G = G_{max}(1 + ([substrate]/K_m))^{-1}, \quad (4)$$

where G_{max} is the upper limit of channel conductance at high substrate concentrations and K_m is the concentration at half-maximal conductance.

Table 1. Determination of association constants for phosphate ion species

Cation	ΔpH	K (M^{-1})
Na^+	0.23	3.5 (3.5)
K^+	0.20	3.0 (3.1)
Cs^+	0.10	1.3
Na^+	0.21	3.5
Cs^+	0.12	1.6
Tris$^+$	−0.06	0

The association constant, K, was determined as described in Methods. K describes the degree of binding between the cation and the divalent form of P_i (see eqn (9)). In the first three rows ΔpH is the difference between the pK_a for P_i (6.92) and the midpoint of a titration in the presence of 200 mM halide salts (pK_a − pH$_t$) and is related to K by eqn (6). The values in parentheses were determined by Smith & Alberty (1956). In the last three rows ΔpH is the fall in pH upon addition of 200 mM cations to 20 mM P_i solutions. These latter measurements of K are not as reliable as those carried out at constant ionic strength because the change in ionic strength alone is likely to produce some change in pH when cations are added to the bath.

The degree of channel inhibition was determined from the ratio of the time-averaged current through the channels measured under control conditions (I) to that in the presence of inhibitor (I_o). Individual data were fitted with eqn (5) to determine the concentration of half-inhibition (K_i) and the Hill coefficient (H):

$$I/I_o = (1 + ([inhibitor]/K_i)^H)^{-1}. \quad (5)$$

Determination of association constant for $CsHPO_4^-$ and $TrisHPO_4^-$

Inorganic phosphate (P_i) ions associate with monovalent cations in solutions giving rise to the three predominant forms of P_i in the pH range 4–10, namely HPO_4^{2-}, $H_2PO_4^-$ and $XHPO_4^-$ where X^+ represents a monovalent cation. The concentrations of these species depend on the pH, the total [X] and [P_i], and the association constants for $XHPO_4^-$ and of $H_2PO_4^-$. The association constants for $NaHPO_4^-$ (3.5 M^{-1}) and $KHPO_4^-$ (3.1 M^{-1}) have been determined previously (Smith & Alberty, 1956). The association constant for $CsHPO_4^-$ (1.3 M^{-1}) was measured here using the same method.

The association constant, K, was determined by measuring the midpoint of the titration of Cs_xP_i (1 mM) with CsOH carried out in solutions containing 200 mM CsCl. Thus the titrations were carried out at near constant ionic strength. Equation (6) relates K to the difference between the pH at the titration midpoint (pH$_t$) and the pK_a for P_i, which is 6.92:

$$K = (10^{pK_p - pH_t} - 1)/[Cs^+]. \quad (6)$$

The titration midpoint and the values of association constants are shown in Table 1. We also carried out titrations using Na^+ and K^+ instead of Cs^+ and obtained values of K for Na^+ and K^+ that were in agreement with those of Smith & Alberty (1956).

It was not possible to use the method of Smith & Alberty (1956) to find the value of K for $TrisHPO_4^-$ because the titration midpoint is obscured by the effects of Tris formation, which has a pK_a of 8.8. We estimated K by another method in which ionic strength was not held constant. K was calculated from the drop in pH upon the addition of 200 mM TrisCl to a solution containing 20 mM $Tris_xP_i$ by solving eqns (7)–(12) (see below). These results are shown in Table 1. Association constants for K^+ and Cs^+ using this method are consistent with those determined at constant ionic strength and the association constant for Tris was

approximately zero, which indicates negligible binding between $Tris^+$ and HPO_4^{2-}. This is consistent with the general trend that weakly charged or large anions show no significant binding with HPO_4^{2-} (Smith & Alberty, 1956).

Concentrations of phosphate species in the pH range 4–10

The relative concentrations of these species can be determined by solving eqns (7)–(12). In the pH range 4–10, the concentrations of H_3O^+, OH^- and PO_4^{3-} are negligibly small. X may exist in either charged or uncharged forms depending on the pH. Thus:

$$[X] = [X^+] \times 10^{pH - pK_X}, \quad (7)$$

where $pK_X = 8.8$ for Tris. Equations (8) and (9) relate the concentrations of the P_i species:

$$[H_2PO_4^-] = [HPO_4^{2-}] \times 10^{pK_P - pH}, \quad (8)$$

$$[XHPO_4^-] = [X^+][HPO_4^{2-}] \times K, \quad (9)$$

where $pK_P = 6.92$ and K is the association constant for cation binding to HPO_4^{2-}. The total ion concentrations in the solution ($[X]_T$ and $[P_i]_T$) are:

$$[X]_T = [XHPO_4^-] + [X^+] + [X], \quad (10)$$

$$[P_i]_T = [HPO_4^{2-}] + [H_2PO_4] + [XHPO_4^-]. \quad (11)$$

Electro neutrality in the solution is described by:

$$[X^+] - 2[HPO_4^{2-}] - [H_2PO_4^-] - [A^-] = 0, \quad (12)$$

where $[A^-]$ is the concentration of additional anions.

Rationale for the choice of cations

We chose $choline^+$, Cs^+, Na^+ and $Tris^+$ as the cations to be used in these experiments. $Choline^+$ and $Tris^+$ were used because they do not permeate the SR K^+ channel, thus obviating the problem of current signals from the SR K^+ channels confusing the anion channel recordings (Coronado & Miller, 1982). In addition, $Tris^+$ was of interest because it does not bind with P_i to form significant concentrations of $TrisHPO_4^-$ (see Table 1 for association constants). Hence channel conductance in the presence of P_i solutions with $Tris^+$ as the cation could be interpreted in terms of fewer ion species than with Cs^+, Na^+ or K^+. Cs^+ was used to test for a possible $XHPO_4^-$ component to P_i transport. Cs^+ was more convenient choice of cation than Na^+ and K^+ because Cs^+ has 10–20 times lower conductance in the SR K^+ channels than Na^+ and K^+ (Cukierman *et al.* 1985). Thus any Cs^+ current through the SR K^+ channels in these experiments would have been relatively small (< 0.5 pA). Although the calcium release channels in the SR have a high conductance to Cs^+ they did not present a problem in this study because (1) anion channels were frequently incorporated into the bilayer without calcium release

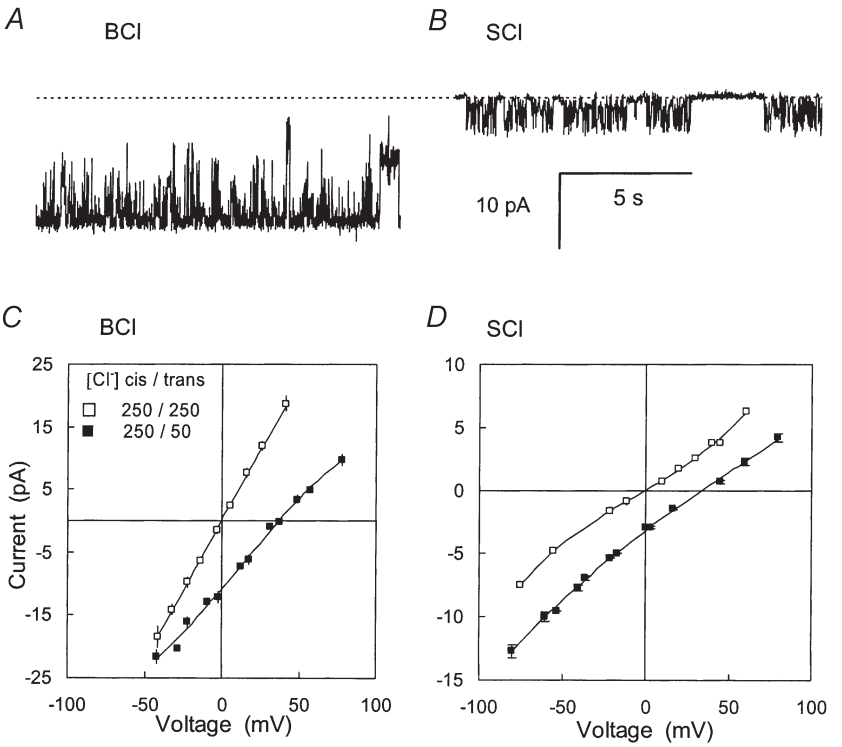

Figure 1. The conductance of anion channels from rabbit SR incorporated into lipid bilayers

A, recording of a single BCl channel in 250/50 mM (*cis/trans*) choline-Cl solutions at −40 mV (*cis* potential) with a slope conductance of 250 pS. The dashed line shows zero current. Scale bars apply to both *A* and *B*. *B*, a single SCl channel with a slope conductance of 80 pS recorded under conditions described in *A*. *C* and *D*, mean current–voltage (*I–V*) data for BCl and SCl channels separating different Cl^- solutions (using Cs^+ or $choline^+$ as the cation. Error bars indicate standard error of the mean voltage and current for each data point. Error bars are frequently obscured by the symbols. *C*, ■, BCl channels in 250/50 mM Cl^- (*cis/trans*, $n = 6$). The conductance, G, and reversal potentials, V_r, are 260 pS and 37 mV. □, BCl channels in 250/250 mM Cl^- (*cis/trans*, $n = 5$), $G = 445$ pS and $V_r = 0$ mV. *D*, ■, SCl channels in 250/50 mM Cl^- (*cis/trans*, $n = 7$), $G = 106$ pS and $V_r = 33$ mV. □, SCl channels in 250/250 mM Cl^- (*cis/trans*, $n = 3$), $G = 90$ pS and $V_r = 0$ mV.

channels, (2) in the presence of 1 mM Ca^{2+} in the cytoplasmic (*cis*) bath the calcium release channels in skeletal muscle are strongly inhibited, and (3) cation channel signals were easily distinguished from anion channels by their conductance and reversal potential. Na^+ was also used as a cation because it is present in muscle and therefore the permeabilities of Na_xP_i complexes are important to P_i transport *in vivo*. However, because Na^+ passes through the SR K^+ channels we had to use Cs^+ on the opposite side of the membrane to the P_i solution to block these channels.

RESULTS

Chloride conductance and selectivity of SCl and BCl channels

As their name suggests the SCl and BCl channels have previously been characterised in terms of their ability to pass Cl^-. The characteristic Cl^- conductance and gating behaviour of BCl and SCl channels are shown in Fig. 1*A* and *B* and their current–voltage (*I–V*) characteristics are shown in Fig. 1*C* and *D*. The BCl channels frequently underwent transitions between fully open and subconductance states while complete channel closures were uncommon. The *I–V* characteristics of the BCl and SCl channels where measured using Cs^+ or choline$^+$ as the cation and were found to be independent of the cation species. In symmetric 250 mM Cl^- the *I–V* curve for the BCl channel was linear with a conductance of 445 pS. In 250 mM/50 mM Cl^- (*cis*/*trans*) the *I–V* curve for the BCl channel has a conductance is 260 pS with a V_r of 37 mV giving permeability ratios $P_{choline}/P_{Cl}$ and P_{Cs}/P_{Cl} of ~0. The SCl channels showed clear burst activity separated by closed periods lasting several seconds. Within bursts the channel opened to a range of subconductance states with the highest conductance states being most commonly observed. In symmetric 250 mM Cl^- the *I–V* curve for the SCl channel was slightly non-linear with an average conductance of 90 pS ($n = 5$) between −40 and +40 mV. In 250 mM/50 mM Cl^- (*cis*/*trans*, $n = 6$) the SCl channel had a conductance of 106 pS and a reversal potential (V_r) of 33 mV, giving permeability ratios for $P_{choline}/P_{Cl}$ and P_{Cs}/P_{Cl} of less than 0.04.

Phosphate conductance of SCl and BCl channels

We investigated the possibility that the P_i flow through the SCl and BCl channels was sufficiently large to produce a detectable current flow. This was done for the SCl channels by subjecting them to fast exchanges between cytoplasmic solutions containing either Cl^- or P_i anions, using local perfusion (Laver & Curtis, 1996). Since continuous changes in the conductance of a single channel were observed (e.g. Fig. 2*A*) it was clear that the same SCl channel had a significant conductance to both Cl^- and P_i. The P_i conductance of BCl channels was demonstrated in records like the one shown in Fig. 2*B*, which was obtained from a bilayer containing 10 BCl channels. The number of channels was determined at the beginning and end of the experiments from their total conductance in the presence of 250 mM choline-Cl (*cis*) and 100 mM Tris-Hepes (*trans*) (not shown). During the experiment the *cis* solution was replaced by 100 mM Tris-Hepes using local perfusion (see above). Addition of 50 mM $Tris_xP_i$ to the *trans* bath produced a 5 pA current.

The mean data for P_i conductance in the SCl and BCl channels over a range of membrane potentials and concentrations is shown in Fig. 3*A* and *B*. The *I–V* characteristic of the SCl channels in symmetric 200 mM

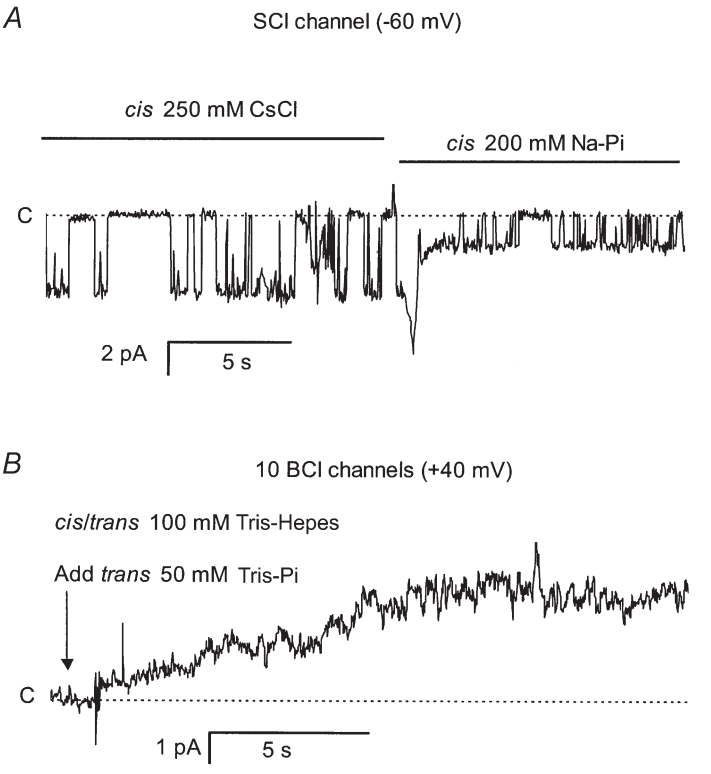

Figure 2. P_i permeates SCl and BCl channels

A, SCl channel openings are downward steps from each baseline (dashed lines labelled C). The SCl channel was initially recorded in CsCl solutions (250/50 mM *cis*/*trans*, left) at −60 mV (net Cl^- flow *cis* to *trans*). A 200 mM Na_xP_i solution was continuously squirted onto the bilayer after 12 s, which replaced Cl^- near the bilayer within ~1 s. The current transient at the time of the solution exchange is an artifact of the exchange process. The current on the right is due to P_i flow from *cis* to *trans*. Clearly the same SCl channel passed both P_i and Cl^- currents. *B*, P_i current through 10 BCl channels in a bilayer. The channels were initially detected with 250 mM choline-Cl (*cis*) and 100 mM Tris Hepes (*trans*) at +40 mV; openings are upward steps from the baseline. The *cis* solution was replaced by 100 mM Tris-Hepes using local perfusion, thus removing all permeant ions in the vicinity of the channels. At the beginning the trace (arrow) 50 mM $Tris_xP_i$ was added to the *trans* bath, which induced a 5 pA current over several seconds as the P_i aliquot mixed with the bath.

Na_xPi (Fig. 3*A*) exhibits a P_i conductance of 16 pS at 0 mV. The channel conductance showed a saturating dependence on $[P_i]$ (Fig. 3*B*). Least squares fits of eqn (4) to the data showed a half-maximum at 64 ± 19 mM P_i and a maximum conductance of 22 ± 2 pS. Saturation was less pronounced for BCl channels. The fit of eqn (4) indicated a half-maximum at 450 ± 280 mM P_i and a maximum conductance of 160 ± 70 pS.

The permeant P_i species

Since P_i can exist in several different forms, it was of interest to determine which form passes predominantly through the channels. Phosphate ions in these experiments and in muscle are predominantly a mixture of three species, namely HPO_4^{2-}, $H_2PO_4^-$ and $XHPO_4^-$ where X^+ represents a monovalent cation. The relative concentrations of these species depend on the pH and monovalent cation concentration. In muscle, the mole ratio concentrations of these species at rest and during fatigue are $[HPO_4^{2-}] = 0.8$ and 14 mM, $[H_2PO_4^-] = 0.2$ and 18 mM and $[(Na+K)HPO_4^-] = 0.4$ and 8 mM (at rest total $[P_i] = 1.4$ mM, $[Na^+] + [K^+] = 150$ mM, pH = 7.18 and during fatigue $[P_i] = 40$ mM, pH ~6.5; Godt & Maughan 1988; Godt & Nosek 1989).

We investigated the permeability of SCl and BCl channels to HPO_4^{2-}, $H_2PO_4^-$and $XHPO_4^-$ where X represents Cs^+,

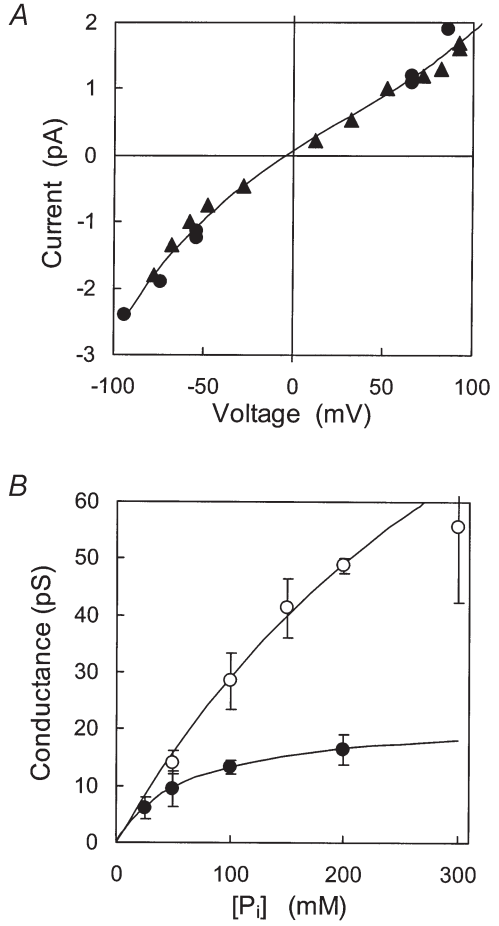

Figure 3. The conductance of SCl and BCl channels to P_i

A, ●, ▲, current–voltage data from two SCl channels, each shown with different symbols, with *cis* and *trans* 200 Na_xP_i. *B*, ●, dependence of SCl channel conductance at −60 mV on *cis* $[Tris_xP_i]$ with *trans* 25 mM $Tris_xP_i$ ($n = 8$). ○, dependence of BCl channel conductance at + 40 mV on *trans* $[Tris_xP_i]$ with *cis* 250 mM choline-Cl ($n = 7$). Error bars show standard error of the mean. Continuous lines show fits of the Michaelis-Menten equation (eqn (4)) to the individual data comprising the mean; SCl data, $G_{max} = 22 \pm 2$ pS, $K_m = 64 \pm 19$ mM; BCl data, $G_{max} = 160 \pm 70$ pS, $K_m = 450 \pm 280$ mM.

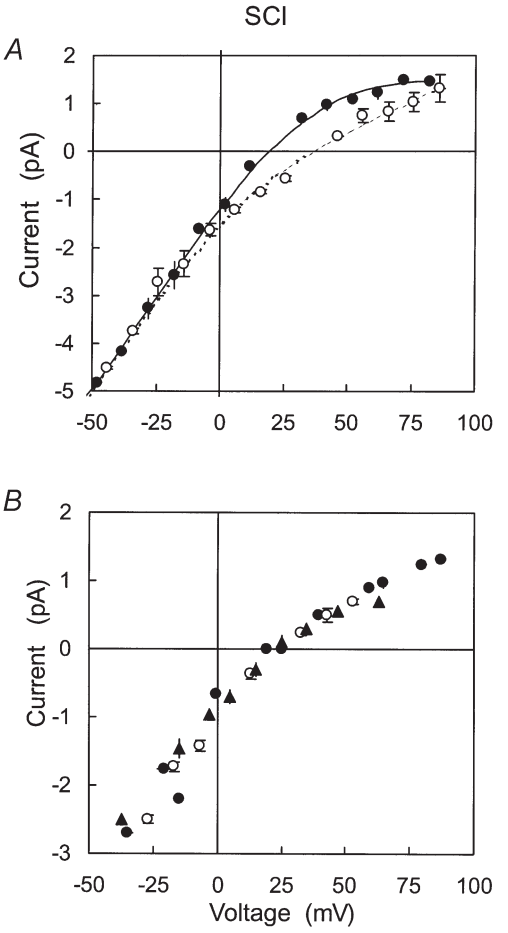

Figure 4. The selectivity of SCl channels to P_i solutions at different pH and in the presence of different cations

A, the *cis* bath contains 250 mM CsCl with *trans* solutions containing: ●, 50 mM Cs_xP_i, pH 7.24, $V_r = 19$ mV ($n = 4$); ○, 50 mM Cs_xPi (pH 7.24) + 200 mM $CsCH_3O_3S$, $V_r = 36$ mV ($n = 3$). The concentrations of each P_i species are given in Table 2. *B*, *I–V* data for SCl channels joining solutions containing 250 mM choline-Cl (*cis*) and *trans* solutions containing: ▲, 200 mM $Tris_xP_i$, pH 7.4, $V_r = 23$ mV ($n = 2$); ○, 250 mM $Tris_xP_i$, pH 6.5, $V_r = 24$ mV ($n = 2$); ●, or 200 mM Na_xP_i, pH 7.4, $V_r = 21$ mV ($n = 2$).

Table 2. Current reversal potentials for SCl channels

	cis ion concentration (mM)	*trans* ion concentration (mM)	Permeant ion species Concentration, activity (mM)			V_r (mV)
1	250 CsCl	50 Cs_xP_i pH 7.24	$[HPO_4^{2-}] = 34, 10$;	$[H_2PO_4^-] = 12, 9$;	$[CsHPO_4^-] = 4, 3$	19 ± 3 (4)
2	250 CsCl	50 Cs_xP_i + 200 $CsCH_3O_3S$ pH 7.24	$[HPO_4^{2-}] = 28, 5$;	$[H_2PO_4^-] = 12, 8$;	$[CsHPO_4^-] = 10, 7$	36 ± 3 (3)
3	250 Cl^-*	200 $Tris_xP_i$ pH 7.4	$[HPO_4^{2-}] = 160, 22$;	$[H_2PO_4^-] = 40, 24$		23 ± 3 (2)
4	250 choline-Cl	250 $Tris_xP_i$ pH 6.5	$[HPO_4^{2-}] = 84, 13$;	$[H_2PO_4^-] = 166, 104$		24 ± 3 (2)
5	250 Cl^-*	200 Na_xP_i pH 7.4	$[HPO_4^{2-}] = 88, 15$;	$[H_2PO_4^-] = 22, 14$;	$[NaHPO_4^-] = 90, 57$	21 ± 3 (2)
6	250 Cl^-*	250 $MgSO_4$	$[SO_4^{2-}] = 100,16$;	$[Cl^-] = 250, 167$		11 ± 2 (8)
7	250 choline-Cl	250 CsBr	$[Br^-] = 250, 167$			5 ± 3 (5)
8	250 choline-Cl	250 CsI	$[I^-] = 250, 167$			6 ± 3 (2)

The concentrations of each P_i species were calculated using the equations and association constants given in Methods. Ion activities were calculated from ionic concentrations using eqn (3). Data are given as mean ± S.E.M. * Cations were either Cs^+ or choline$^+$ and the Cl^- activity is 167 mM. Values of n are given in parentheses.

Table 3. Current reversal potentials for BCl channels

	cis ion concentration (mM)	*trans* ion concentration (mM)	Permeant ion species Concentration, activity (mM)			V_r (mV)
1	250 CsCl	50 Cs_xP_i; pH 7.24	$[HPO_4^{2-}] = 34, 10$;	$[H_2PO_4^-] = 12, 9$;	$[CsHPO_4^-] = 4, 3$	52 ± 4 (4)
2	250 CsCl	50 Cs_xP_i + 200 $CsCH_3O_3S$ pH 7.24	$[HPO_4^{2-}] = 28, 5$;	$[H_2PO_4^-] = 12, 8$;	$[CsHPO_4^-] = 10, 7$	54 ± 4 (4)
3	250 CsCl	50 Cs_xP_i; pH 6.5	$[HPO_4^{2-}] = 15, 5$;	$[H_2PO_4^-] = 30, 23$;	$[CsHPO_4^-] = 5, 4$	58 ± 4 (4)
4	250 choline-Cl	200 $Tris_xP_i$; pH7.4	$[HPO_4^{2-}] = 160, 22$;	$[H_2PO_4^-] = 40, 24$		50 ± 4 (7)
5	250 choline-Cl	250 $Tris_xP_i$; pH6.5	$[HPO_4^{2-}] = 84, 13$;	$[H_2PO_4^-] = 166, 104$		50 ± 4 (4)
6	200 Na_xP_i; pH 7.4	250 choline-Cl	$[HPO_4^{2-}] = 88, 15$;	$[H_2PO_4^-] = 22, 14$;	$[NaHPO_4^-] = 90, 57$	-36 ± 3 (4)
7	250 Cl^-	250 $MgSO_4$	$[SO_4^{2-}] = 100, 16$;	$[Cl^-] = 250, 167$		55 ± 4 (8)
8	250 choline-Cl	250 CsBr	$[Br^-] = 250, 167$			6 ± 3 (5)
9	250 choline-Cl	250 CsI	$[I^-] = 250, 167$			7 ± 3 (4)

Ion concentrations and activity were calculated as described in the caption to Table 2.

Na^+ and $Tris^+$. In order to obtain the permeabilities of the three P_i species it was necessary to measure reversal potentials of the anion channels at different pH and/or $[X^+]$: conditions in which the relative concentrations of the P_i species were different (see Methods). The concentrations of each ion species (Tables 2 and 3) were calculated using eqns (7)–(12) (see Methods) and association constants given in Table 1. By applying the constant field equation to each of these situations it was possible to calculate the ion permeabilities for the individual P_i species. The effects of altering the relative concentrations of P_i species on the I–V characteristics of SCl channels are shown in Fig. 4. In Fig. 4*A*, the addition of $CsCH_3O_3S$ to the *trans* chamber reduced $[HPO_4^{2-}]$ and increased $[CsHPO_4^-]$ (see Tables 1 and 2). The I–V characteristic of the SCl channel was significantly affected by the addition of cations to the *trans* bath with a shift in the reversal potential from 19 to 36 mV (Table 2, rows 1 and 2). Solving the constant field equation for the permeability ratios of each ion species gives the selectivity sequence $HPO_4^{2-} > Cl^- > H_2PO_4^-$ and $CsHPO_4^-$ (Table 4). The same selectivity sequence was independently obtained at ~200 mM P_i by comparing the I–V characteristics obtained at pH 7.4 and 6.5 (Fig. 4*B*). Decreasing the pH reduced the relative concentration of HPO_4^{2-} yet did not significantly change V_r (Table 2, rows 3–5). Although the permeability selectivity sequence with ~200 mM P_i or 50 mM P_i was the same, the degree of specificity for the different ions was less at higher concentrations (Table 4). Thus the SCl channels are permeable mainly to the divalent HPO_4^{2-} and the specificity is more pronounced at lower $[P_i]$.

The effects of manipulating the relative concentrations of P_i species on BCl channels were also investigated. The effects of changing pH and $[Cs^+]$ in the P_i solutions on the BCl channel I–V characteristic are shown in Fig. 5. In contrast to results above for the SCl channel, the I–V characteristic of the BCl channel was little affected by the addition of $CsCH_3O_3S$ to the *trans* bath, which shifted V_r from 52 to 54 mV (Table 3, rows 1–3). According to the constant field equation this indicates that the BCl channel is less selective for HPO_4^{2-} than the SCl channel. Decreasing the pH of the Cs_xP_i solution in the *trans* bath from 7.24 and 6.5 shifted V_r from 52 to 58 mV (Fig. 5). The constant field equation gives the selectivity sequence $NaHPO_4^- > Cl^- > HPO_4^{2-} > H_2PO_4^-$ (Table 4). A slightly different selectivity sequence ($Cl^- > NaHPO_4^- > HPO_4^{2-} > H_2PO_4^-$) was obtained at higher P_i, ~200 mM, by comparing the I–V characteristics obtained at pH 7.4 and 6.5 (Table 3, rows

Table 4. Anion permeabilities in SCl and BCl channels

Anion (Y)	SCl channel P_Y/P_{Cl}	BCl channel P_Y/P_{Cl}
50 mM P_i		
HPO_4^{2-}	3.0 ± 0.4 [a]	0.4 ± 0.2 [g]
$H_2PO_4^-$	0 [a]	0.1 ± 0.1 [g]
$CsHPO_4^-$	0 [a]	1.7 ± 0.2 [g]
~200 mM P_i		
HPO_4^{2-}	0.9 ± 0.2 [b]	0.3 ± 0.2 [h]
$H_2PO_4^-$	0.3 ± 0.2 [b]	0.1 ± 0.1 [h]
$NaHPO_4^-$	0.4 ± 0.2 [c]	0.5 ± 0.2 [i]
SO_4^{2-}	3.0 ± 0.2 [d]	< 0.3 [j]
Br^-	0.7 ± 0.2 [e]	0.8 ± 0.1 [k]
I^-	0.8 ± 0.1 [f]	0.8 ± 0.1 [l]

Table 4. Permeability (relative to Cl^-) was calculated from V_r and known activities of ions in the bathing solutions (see Tables 2 and 3) using the constant field equation (eqn (2)). Assumed values of cation permeability over the range 0 to 0.05 had no significant effect on the predicted anion permeability.
[a]Calculated from Table 2 (rows 1 and 2) assuming permeabilities for Cs^+ and $CH_3O_3S^-$ equal zero.
[b]Calculated from Table 2 (rows 3 and 4) assuming $Tris^+$ permeability equals zero.
[c]Calculated from Table 2 (rows 3–5) assuming Na^+ permeability equals zero.
[d]Calculated from Table 2 (row 6) assuming permeabilities for Mg^{2+} and $choline^+$ equal zero.
[e]Calculated from Table 2 (row 7) assuming permeabilities for $choline^+$ and Cs^+ equal zero.
[f]Calculated from Table 2 (row 8) assuming permeabilities for $choline^+$ and Cs^+ equal zero.
[g]Calculated from Table 3 (rows 1–3) assuming permeabilities for Cs^+ and $CH_3O_3S^-$ equal zero.
[h]Calculated from Table 3 (rows 4 and 5) assuming $Tris^+$ permeability equals zero.
[i]Calculated from Table 3 (rows 4–6) assuming Na^+ permeability equals zero.
[j]Calculated from Table 3 (row 7) assuming permeabilities for $choline^+$ and Cs^+ equal zero.
[k]Calculated from Table 3 (row 8) assuming permeabilities for $choline^+$ and Cs^+ equal zero.
[l]Calculated from Table 3 (row 9) assuming permeabilities for $choline^+$ and Cs^+ equal zero.

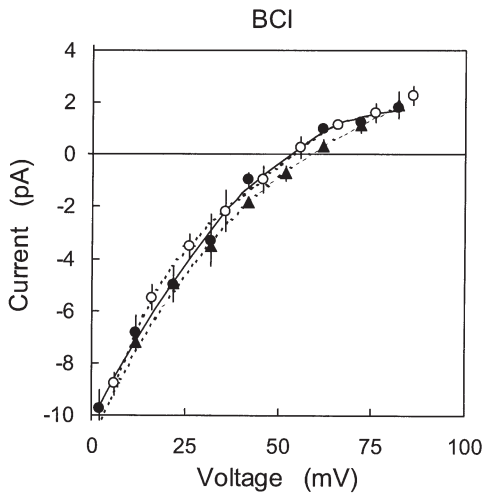

Figure 5. The selectivity of BCl channels to P_i solutions at different pH and in the presence of different Cs^+ concentrations

The concentrations of each P_i species are given in Table 3. The *cis* bath contains 250 mM CsCl with *trans* solutions containing: ●, 50 mM Cs_xP_i, pH 7.24, $V_r = 52$ mV ($n = 4$); ○, 50 mM Cs_xP_i + 200 mM $CsCH_3O_3S$, pH 7.24, $V_r = 54$ mV ($n = 4$); ▲, 50 mM Cs_xP_i, pH 6.5, $V_r = 58$ mV ($n = 4$).

4–6). In either case HPO_4^{2-} is not the main permeant form of P_i in the BCl channel.

The valence selectivity of these channels was also investigated in another way by measuring the channel permeability to I^- and Br^- and SO_4^{2-} in the SCl and BCl channels. These ions form fewer ion species than P_i. Figure 6 shows the *I–V* characteristics of SCl and BCl channels with solutions containing Cl^- (*cis*) and either I^- or Br^- (*trans*) and with either Cs^+ or $choline^+$ as the cation. Current reversal potentials were found to be in the range 0–10 mV (Table 2, rows 7 and 8 and Table 3, rows 8 and 9). The conductance and relative permeabilities for both channels show little specificity between the monovalent anions, $Cl^- > I^- > Br^-$ (see Table 4). In contrast to the monovalent anions, SCl and BCl channels differed in their ability to conduct divalent SO_4^{2-} (Fig. 7, cf. Table 2, row 6 and Table 3, row 7). For the SCl channel with 250 mM $MgSO_4$ (*cis*) and 250 mM Cl^- (*trans*), V_r was 11 mV, indicating a 3-fold selectivity for SO_4^{2-} over Cl^-. The SCl channel conductance in 250 mM $MgSO_4$ (*cis*/*trans*) was 60 pS (Fig. 7, filled symbols). In marked contrast, the V_r for the BCl channel (Fig. 7) under similar conditions was ~55 mV, which was closer to the equilibrium potential for Cl^- (i.e. > 100 mV) indicating selectivity for Cl^-. The gating pattern associated with the BCl channel passing

Cl^- (e.g. Fig. 1*A*) was never resolved above the background noise when SO_4^{2-} was the permeant ion indicating that the SO_4^{2-} conductance was very small (< 10 pS). Consequently a precise determination of V_r, and hence P_{SO4}/P_{Cl}, was not possible for the BCl channel. However we were able to obtain an upper estimate for P_{SO4}/P_{Cl} of 0.3. Thus the BCl channel is a monovalent anion channel whereas the SCl is selective for divalent ions over monovalent ions.

In summary, the data give an overall picture of P_i permeation in which the SCl channel is primarily permeable to the divalent HPO_4^{2-} and not the monovalent $H_2PO_4^-$ or $XHPO_4^-$ while, in contrast, the BCl channel is impermeable to HPO_4^{2-}. The mechanism for P_i permeation in the BCl channel is not clear. Reversal potential measurements in Fig. 5 suggest that $CsHPO_4^-$ is the main permeant form of P_i in the BCl channels. However, this is difficult to reconcile with the fact that BCl channels also conduct P_i in the presence of $Tris_xP_i$ (e.g. see Figs 2 and 3). In these solutions the $TrisHPO_4^-$ concentration would be very low and in any case $TrisHPO_4^-$ is likely to be too large to fit through the pore (the BCl channel was found to be impermeable to large anions such as $CH_3O_3S^-$ and $Hepes^-$). This suggests that the constant field equation does not adequately describe ion permeation in these channels under all conditions.

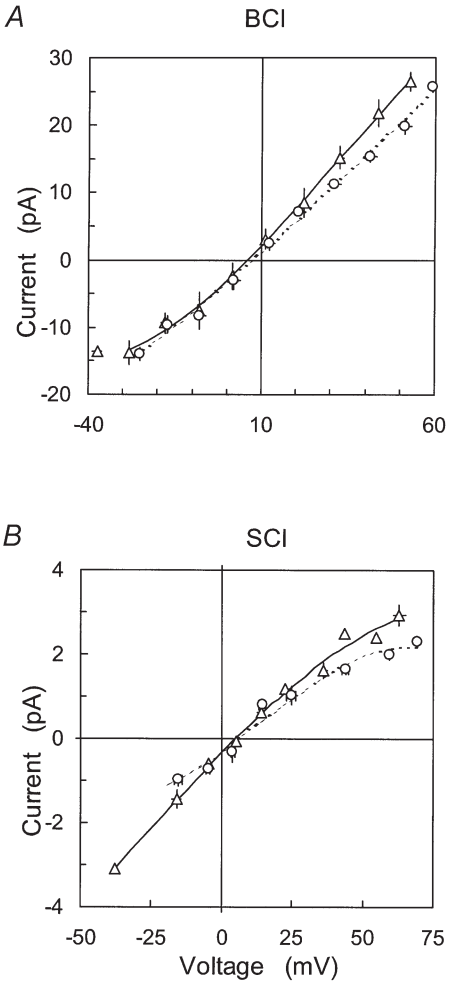

Figure 6. The mean *I–V* characteristics of SCl and BCl channels separating equimolar ionic solutions

A, BCl channels in *cis* solutions containing 250 mM choline-Cl and with *trans* solutions containing: ○, 250 mM CsI, $G = 440$ pS and $V_r = 7$ mV ($n = 4$); △, 250 mM CsBr, $G = 580$ pS and $V_r = 6$ mV ($n = 5$). *B*, SCl channels in *cis* solutions containing 250 mM choline-Cl and with *trans* solutions containing: ○, 250 mM CsI, $G = 43$ pS and $V_r = 6$ mV ($n = 2$); △, 250 mM CsBr, $G = 54$ pS and $V_r = 5$ mV ($n = 4$).

Anion channel inhibition by phosphonocarboxylic acids

The SR P_i flux is inhibited by the phosphonocarboxylic acids (Stefanova *et al.* 1991*b*; Posterino & Fryer, 1998). Two acids from this family with significantly different inhibiting potencies were used here, namely phosphonoformic acid (PFA) and phenylphosphonic acid (PhPA). PFA is 4-fold more potent in inhibiting SR P_i flux than PhPA. Both phosphonocarboxylic acids reduced the Cl^- current through SCl and BCl channels (Fig. 8). The phosphonocarboxylic acids acted predominantly by reducing the open channel conductance. PFA also slightly decreased the open probability of the SCl channel. Both PFA and PhPA increased the root mean square noise on channel openings relative to the open channel current indicating a 'flicker'-block of the channel by these acids. The concentration dependence of inhibition under a variety of conditions is shown in Fig. 9*A* and *B*. PhPA inhibition of BCl channels was voltage dependent (being greater at negative potentials) and alleviated by increasing *cis* $[Cl^-]$, while PFA block was voltage-

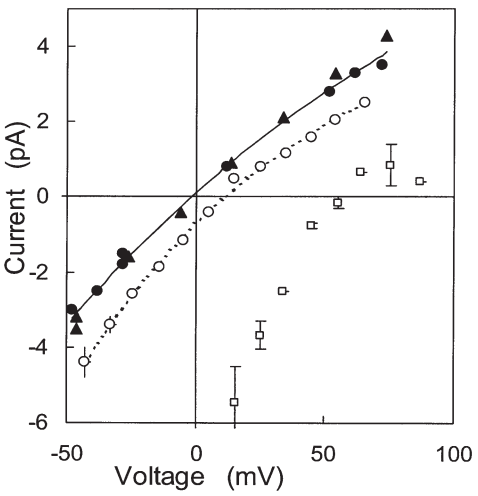

Figure 7. Mean *I–V* characteristics of SCl and BCl channels in the presence of SO_4^{2-}

□, BCl channels with 250 mM CsCl (*cis*) and 250 mM $MgSO_4$ (*trans*) $V_r = 55$ mV ($n = 2$). ▲, ●, two SCl channels in *cis* and *trans* 200 mM Na_xP_i (each shown with different symbols) $G = 60$ pS. ○, SCl channels with 250 mM $MgSO_4$ *cis* and 250 mM choline-Cl *trans*, $V_r = 11$ mV ($n = 8$).

Table 5. Block of BCl and SCl channels by phosphonocarboxylic acids

		BCl		SCl
Acid	*cis* $[Cl^-]$ (mM)	K_i (−40 mV)	K_i (0 mV)	K_i (−40 mV)
PhPA	250	20 ± 2 (11)	60 ± 11 (9)	30 ± 4 (3)
PhPA	125	10 ± 1.2 (3)	—	—
PhPA	63	5 ± 2 (3)	—	—
PFA	250	23 ± 3 (6)	21 ± 2 (6)	6.5 ± 1.1 (3)

Block of BCl and SCl channels by phosphonocarboxylic acids from bilayer experiments showing the concentration of acid in the *cis* bath that produced a 50% reduction in Cl^- currents (concentrations in mM). Numbers of observations are given in parentheses.

independent (Table 5). PFA was a stronger blocker of SCl channels than BCl channels (i.e. PFA blocked SCl channels with higher affinity than PhPA, Table 5). The errors on the Hill coefficient estimates were typically 0.2–0.3 and in all cases the Hill coefficients were not significantly different from unity (not shown).

Anion channel inhibition by DIDS

Both BCl and SCl channels frequently incorporated into bilayers in the same fusion event. These bilayers could not be used to study either channel type using Cl^- based solutions. However, when SO_4^{2-} was the major anion, such bilayers could be used to examine SCl channel activity, because no detectable current flowed through the BCl channels. Therefore the effect of DIDS on SCl channel activity was examined in $MgSO_4$ solutions. The presence of Mg^{2+} had the added advantage of inhibiting ryanodine receptors so they did not interfere with SCl channel recordings.

DIDS is a potent inhibitor of anion channels and the P_i efflux from SR vesicles (Campbell & MacLennan, 1980). We found that addition of 20–60 μM DIDS to the *cis* (cytoplasmic) bath caused total inhibition of SCl channel conductance for SO_4^{2-} within 30s of application ($n = 5$, e.g. Fig. 10*A*) whereas DIDS (*cis* 0.1 to 1 mM) produced only 14 ± 6% inhibition of the BCl channel conductance for Cl^- after several minutes of exposure ($n = 4$, e.g. Fig. 10*B*).

DISCUSSION

In this study we have shown that the BCl and SCl channels pass inorganic phosphate ions and thus identified the first candidates for the P_i transport mechanism in the SR. Previous studies have determined that the BCl and SCl channels are differently regulated by membrane potential and the cytoplasmic milieu (see Introduction). We find that BCl and SCl channels have distinct ion selectivities, the SCl being primarily a divalent anion channel whereas the BCl channel is

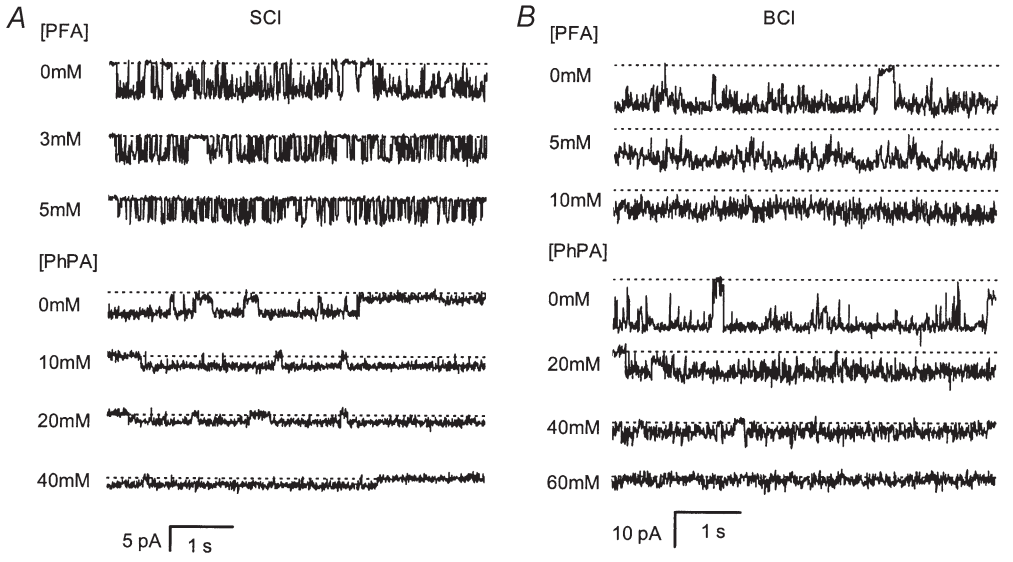

Figure 8. Inhibition of BCl and SCl channels by phosphonoformic acid (PFA) and phenylphosphonic acid (PhPA)

A, two separate experiments in which different SCl channels were inhibited by PFA (top three traces) and PhPA (bottom four traces). PFA inhibition was measured in the presence of 250/50 mM CsCl (*cis*/*trans*) at −60 mV and PhPA inhibition was measured in 250 mM choline-Cl (*cis*) and 50 mM $Tris_xP_i$ + 100 mM Tris-Hepes (*trans*) at −40 mV. The channel conductance is reduced in the presence of either acid. *B*, two experiments in which different BCl channels were inhibited by PFA (top three traces) and PhPA (bottom four traces). PFA inhibition was measured in the presence of 250 mM choline-Cl (*cis*) and 50 mM $Tris_xP_i$ + 200 mM Tris-Hepes (*trans*) at −40 mV and PhPA inhibition was measured in 250 mM choline-Cl (*cis*) and 200 Tris-Hepes (*trans*) at −40 mV.

primarily a monovalent anion channel. P_i-conducting ion channels have not previously been reported in muscle although a phosphate-permeable anion channel has recently been reported in the Golgi bodies of liver cells (Nordeen *et al.* 2000). The conductance and selectivity of the BCl channel for anions other than P_i was consistent with a previous report (Tanifuji *et al.* 1987).

Our key finding is that P_i flows through at least one of the anion channels of the SR. The evidence for this comes from a direct measurement of single channel current in the presence of P_i solutions. We have also inferred relative anion permeability from measurements of reversal potential. However, some caution should be exercised in interpreting these values. First, while our results provide reliable data, the available theories to interpret reversal potentials are not exact. The assumptions inherent in the constant field equation, while valid for whole cell currents, are not strictly applicable to individual channels where ion flows may not be independent. Therefore ion permeability values merely provide a condensed description of the reversal potential data. Secondly, for relative ion permeabilities a high specificity for P_i over other anions might not be an important prerequisite for a P_i transporter. Readily diffusible anions in the resting muscle cytoplasm consisted mainly of adenine nucleotides (~6–8 mM), chloride (2–5 mM), phosphocreatine (48 mM), lactate (1.5 mM), amino acids (1 mM) glycolytic intermediates (< 4 mM), bicarbonate (< 8 mM) and inorganic phosphates (1–5 mM) (Godt & Maughan, 1988). During prolonged exercise the cytoplasmic P_i rises to 20–40 mM at the expense of phosphocreatine so that P_i becomes the dominant diffusible anion in the cytoplasm. Thus ion channels with only moderate specificity for P_i could pass substantial P_i fluxes under these conditions.

Contributions of SCl and BCl channels to SR P_i transport

If the BCl and SCl channels are viable candidates for the physiological P_i transport mechanism then they must be sufficiently permeable to P_i to account for the magnitude of the fluxes seen in muscle. Passive P_i uptake by SR in rat muscle has been estimated as 50 μM s^{-1} (relative to whole fibre volume) with 20 mM cytoplasmic P_i (Fryer *et al.* 1997). An upper estimate of SCl and BCl channel contributions to P_i transport can be made from their P_i conductance and population density. (Channel density in muscle, D, was calculated from the number per SR vesicle, $N = 0.69$ (Smith *et al.* 1986), the radius of each vesicle, $r = 0.14$ μm (Tanifuji *et al.* 1987) and the area of SR membrane per unit volume of muscle fibre $A = 1$ μm^2/μm^3 (Eisenberg, 1982) using the equation: $D = AN/4\pi r^2$). The Constant Field equation predicts that at $V_m = 0$ and 20 mM P_i (where BCl and SCl P_i conductance is similar) a unidirectional P_i current of ~0.05 pA per fully open channel gives a SR transport rate of ~700 μM s^{-1}, more than enough to carry the observed P_i fluxes.

The contributions of SCl and BCl channels to physiological P_i fluxes across the SR membrane may be assessed by comparing activation and inhibition of these channels with activation and inhibition of P_i fluxes. The SR P_i flux is inhibited by phosphonocarboxylic acids; phosphonoformic acid (PFA) being approximately fourfold more potent than phenylphosphonic acid (PhPA) (Stefanova *et al.* 1991*b*). Phosphonocarboxylic acids also reduced Cl^- current through the SCl and BCl channels (Figs 8 and 9). The dependence of inhibition by the acids on voltage and *cis*[Cl^-] indicates that the acids compete with permeant anions for a blocking site

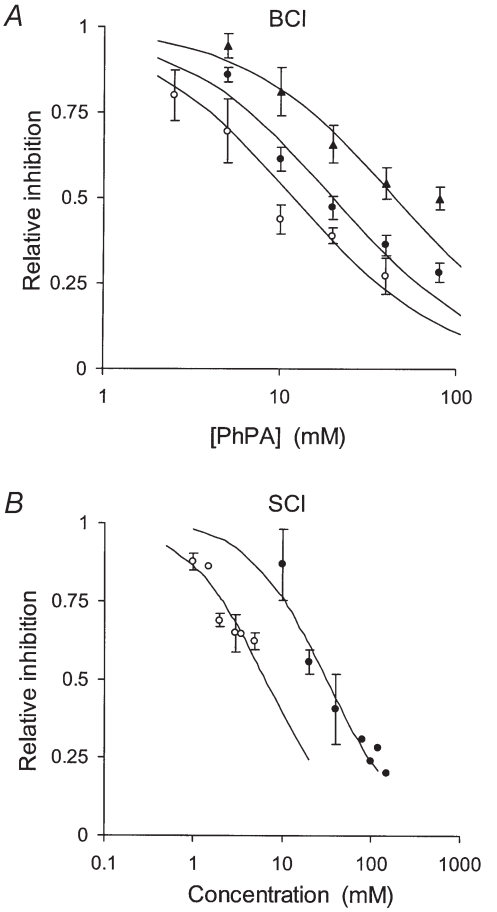

Figure 9. Concentration dependence of cytoplasmic phosphonocarboxylic acid inhibition of BCl and SCl channels

Inhibition was measured from the ratio of the time-averaged current in the presence of acid, and under control conditions. *A*, BCl channel inhibition by *cis* PhPA in the presence of *trans* 100 mM Tris-Hepes and under the following conditions. ▲, *cis* 250 mM choline-Cl, 0 mV ($n = 9$); ●, 250 mM choline-Cl, −40 mV ($n = 11$); ○, 125 mM choline-Cl, −40 mV ($n = 3$). The curves show Hill fits to the data (Hill coefficient = 1). Half-inhibiting concentrations from these fits are given in Table 3. *B*, SCl inhibition by *cis* phosphonocarboxylic acids in the presence of *trans* 100 mM Tris-Hepes and *cis* 250 mM choline-Cl at −40 mV. ○, PFA ($n = 3$); ●, PhPA ($n = 3$).

within the conduction pathway. The ratio of K_i for the two phosphonocarboxylic acids K_i (PhPa)/K_i (PFA) is in the range 1–2 for the BCl channel and 4–5 for the SCl channel (Table 5). This ratio for the SCl channel is more consistent with the relative effects of the acids on SR vesicles. Although the relative K_i values for the phosphonocarboxylic acids on the anion channels were consistent with those for P_i uptake by SR vesicles, their absolute potency for blocking BCl or SCl channels (K_i = 5–50 mM) was lower than that for P_i uptake by the SR (K_i ~1 mM). This discrepancy is most likely to be due to the high [Cl^-] necessary to detect channels in bilayers, since lowering *cis* [Cl^-] toward physiological levels of ~5 mM lowered K_i (Cl^- and phosphonocarboxylic acids act competitively, see above).

Disulfonic stilbenes are potent anion channel inhibitors but unfortunately there are conflicting interpretations of the DIDS effect on SR P_i transport. Direct measurement of P_i efflux from SR vesicles showed that DIDS produced complete inhibition at 50 μM with a half-inhibiting concentration (K_i) of 3 μM (Campbell & MacLennan, 1980). However, P_i release from the SR of skinned fibres, inferred from the P_i-induced decrease in Ca^{2+} release, showed that 100 μM DIDS had no significant effect on P_i transport (Posterino & Fryer, 1998). The reason for the disparate findings may lie in the promiscuous nature of DIDS, which affects a variety of membrane transporters. DIDS is known to strongly activate the Ca^{2+} release channel in the SR (Oba *et al.* 1996; Sitsapesan, 1999) so that indirect estimates of P_i transport from SR Ca^{2+} handling properties might not be valid. Anion channel inhibition by DIDS shown here is consistent with our previous report (Kourie *et al.* 1996*b*) that 8 μM DIDS inhibited the Cl^- conductance of SCl channels but 80 μM DIDS caused only partial inhibition of BCl channels. Thus we find that the effect of DIDS on the SCl channel parallels its effect on P_i transport determined from direct measurements of efflux from SR vesicles.

Cytoplasmic ATP has been shown to inhibit P_i influx but not P_i efflux from the SR (Posterino & Fryer, 1998). BCl channels are not sensitive to ATP (≤ 20 mM, not shown), but SCl channels are sensitive to ATP. The K_i for ATP is 1 mM when 250 mM Cl^- flows through SCl channels from cytoplasm to lumen (influx), whereas 10 mM ATP has no effect when Cl^- flows in the opposite direction (efflux) (Ahern & Laver, 1998). Thus the inhibiting effects of ATP on the SCl channels, not the BCl channels, closely parallels its effects on P_i transport in muscle.

In summary, the P_i conductance and density of SCl and BCl channels suggest that both channel types could sustain the observed P_i fluxes across the SR membrane. However, the pharmacological evidence suggests that the SCl channel is the more likely candidate for the P_i transport mechanism in the SR.

Physiological roles for the SCl and BCl channels

The role of anion channels in the SR is unknown. It had been suggested that their role might be to contribute a Cl^- flux to the counter current during Ca^{2+} release and uptake (Kourie *et al.* 1996*a*,*b*). However, the failure to demonstrate changes in SR [Cl^-] during muscle tetanus (Somlyo *et al.* 1981) and the lack of an effect of Cl^- removal on voltage sensor-activated contraction (Coonan & Lamb, 1998) suggest that Cl^- is not an essential contributor to counter currents. It is more likely that the role of the anion channels is associated with the transport of other relatively permeant anions (e.g. SO_4^{2-} and P_i).

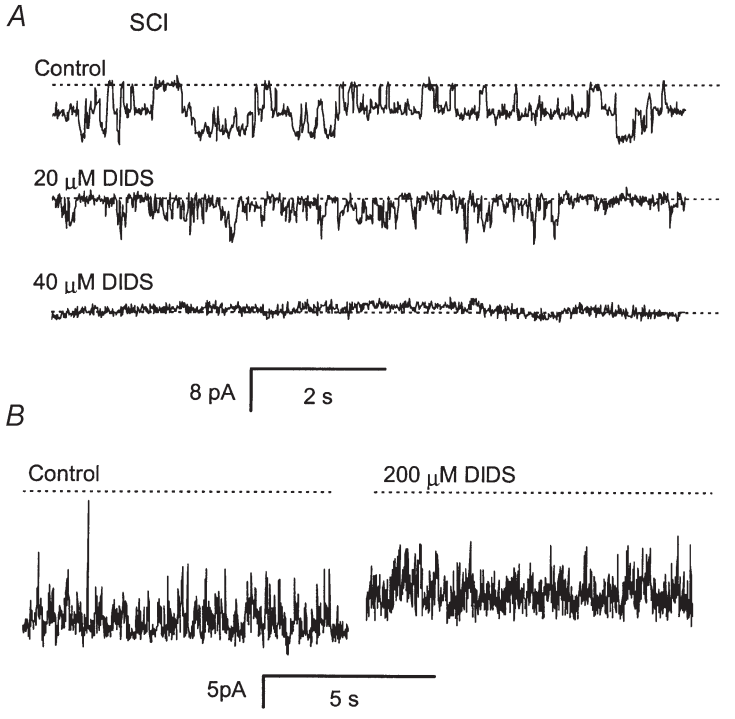

Figure 10. The effect of DIDS in the cytoplasmic bath on the SCl and BCl channels

A, one of five experiments showing two SCl channels in *cis* 250 mM $MgSO_4$ and *trans* 200 mM $Tris_xP_i$ at −60 mV (top trace). The current is carried by SO_4^{2-} flowing from *cis* to *trans*. The channels became substantially inhibited within 20 s of the addition of 20 μM DIDS to the *cis* bath (second trace). Further addition of DIDS totally inhibited the channels within 10 s (bottom trace). *B*, one of four experiments showing a BCl channel in *cis* 250 mM choline-Cl and *trans* 100 mM Tris-Hepes at −40 mV (left trace). The channel showed 20% inhibition after 200 μM DIDS was added to the *cis* bath (right trace).

This is the first report of a high-conductance, SO_4^{2-}-selective ion channel in mammalian membranes (the SCl channel). A SO_4^{2}-conducting channel has recently been reported in plants (Frachisse *et al.* 1999). The physiological significance of the strikingly high SO_4^{2-} permeability of the SCl channel is at present unclear.

The pharmacological evidence weighs against the BCl channel having a significant role in P_i transport across the SR. However, the BCl channel may provide a non-specific anion leak pathway. A physiological role for the SCl channel, and to a small extent the BCl channel, might be to allow P_i to cross the SR membrane and either associate with, or dissociate Ca^{2+} in, the SR lumen. The co-precipitation of Ca^{2+} and P_i in the SR is believed to be a major contributor to failure of Ca^{2+} release and muscle contraction during fatigue from prolonged activity (Fryer *et al.* 1995; Kabbara & Allen, 1999; Dahlstedt *et al.* 2000). The strongest evidence for this hypothesis comes from recent experiments on creatine kinase knock-out mice where cytoplasmic P_i does not increase during intense exercise (Dahlstedt *et al.* 2000). Muscle fibres from these mice were considerably more resistant to fatigue than those from normal mice. Though it is clear that P_i can cross the SR membrane, the main transport mechanism is unknown. The SCl channel is a good candidate for such a transport mechanism since (1) pharmacological agents that alter SR P_i transport have similar effects on the SCl channel and (2) they can sustain the observed P_i fluxes across the SR membrane during normal muscle function (see above) and during fatigue and recovery from fatigue where intracellular pH falls.

The high degree of regulation of the SCl channel by cytoplasmic ligands can be understood if the SR anion channels do play an essential role in regulating P_i transport. Results, here and elsewhere (Kourie *et al.* 1996*a*; Kourie, 1997*a*,*b*; Ahern & Laver, 1998), suggest that SCl channels would be further activated in muscle fatigue by raised cytoplasmic [Ca^{2+}], luminal [P_i] (D. R. Laver, unpublished observations), reduced [ATP] and by increased concentrations of oxidants. Thus the SCl channel would increase the overall permeability of the SR membrane to P_i under conditions of muscle fatigue and ischaemia. This could serve either (1) to reduce the available Ca^{2+} pool under conditions of stress (fatigue or ischaemia) and so have a protective effect in conserving Ca^{2+} stores and reducing muscle output when energy reserves are low or (2) to aid in recovery from fatigue by allowing rapid P_i exit from the SR.

Physiological (0.5–10 mM) [P_i] has been shown to both increase or decrease (depending on the concentration) the size of intracellular Ca^{2+} stores that are rapidly releasable by either ryanodine (Fryer *et al.* 1995, 1997; Posterino & Fryer, 1998; Kabbara & Allen, 1999), InsP_3 (Fulceri *et al.* 1993; Mezna & Michelangeli, 1998) or cADP-ribose (Guse *et al.* 1996), in tissues as diverse as hepatic cells, lymphocytes, platelets, brain and haematoma cells. The presence of an anion channel pathway for P_i into the SR of muscle raises the possibility that this is a general mechanism for P_i movement into and out of Ca^{2+} stores in many cell types.

Ahern, G. P. & Laver, D. R. (1998). ATP inhibition and rectification of a Ca^{2+}-activated anion channel in sarcoplasmic reticulum of skeletal muscle. *Biophysical Journal* **74**, 2335–2351.

Barry, P. H. & Lynch, J. W. (1991). Liquid junction potentials and small cell effects in patch-clamp analysis. *Journal of Membrane Biology* **121**, 101–117.

Brooks, S. P. & Storey K. B. (1992). Bound and determined: a computer program for making buffers of defined ion concentrations. *Annals of Biochemistry* **201**, 119–126.

Campbell, K. P. & MacLennan, D.H. (1980). DIDS inhibition of sarcoplasmic reticulum anion and calcium transport. *Annals of the New York Academy of Sciences* **358**, 328–331.

Chu, A., Dixon, M. C., Saito, A. Seiler, S. & Fleischer, S. (1988). Isolation of sarcoplasmic reticulum fractions referable to longitudinal tubules and junctional terminal cisternae from rabbit skeletal muscle. *Methods in Enzymology* **157**, 36–50.

Coonan, J. R. & Lamb, G. D. (1998). Effect of chloride on Ca^{2+} release from the sarcoplasmic reticulum of mechanically skinned skeletal muscle fibres. *Pflügers Archiv* **435**, 720–730.

Coronado, R. & Miller, C. (1982). Conduction and block by organic cations in a K^+ selective channel from sarcoplasmic reticulum incorporated into planar phospholipid bilayers. *Journal of General Physiology* **79**, 529–547.

Cukierman, S., Yellen, G. & Miller, C. (1985). The K^+ channel of sarcoplasmic reticulum. A new look at Cs^+ block. *Biophysical Journal* **48**, 477–484.

Dahlstedt, A. J., Katz, A., Wieringa, B. & Westerblad, H. (2000). Is creatine kinase responsible for fatigue? Studies of isolated skeletal muscle deficient in creatine kinase. *FASEB Journal* **14**, 982–990.

Duke, A. M. & Steele, D. S. (2000). Characteristics of phosphate-induced Ca^{2+} efflux from the SR in mechanically skinned skeletal muscle fibres. *American Journal of Physiology* **278**, C126–135.

Eisenberg, B. R. (1982). Quantitative ultrastructure of mammalian skeletal muscle. In *Handbook of Physiology*, section 10, *Skeletal Muscle*, ed. Peachey, L. D. & Adrian, R., pp. 73–112. American Physiological Society, Bethesda, MD, USA.

Frachisse, J. M., Thomine, S., Colcombet, J., Guern, J. & Barbier-Brygoo, H. (1999). Sulfate is both a substrate and an activator of the voltage-dependent anion channel of arabidopsis hypocotyl cells. *Plant Physiology* **121**, 253–261.

Fruen, B. R., Mickelson, J. R., Shomer, N. H., Rogher, T. J. & Louis, C. F. (1994). Regulation of the sarcoplasmic reticulum ryanodine receptor by inorganic phosphate. *Journal of Biochemistry* **269**, 192–198.

Fryer, M. W., Owen, V. J., Lamb, G. D. & Stephenson, D. G. (1995). Effects of creatine phosphate and P_i on Ca^{2+} movements and tension development in rat skinned skeletal muscle fibres. *Journal of Physiology* **482**, 123–140.

Fryer, M. W., West, J. M. & Stephenson, D. G. (1997). Phosphate transport into the sarcoplasmic reticulum of skinned fibres from rat skeletal muscle. *Journal of Muscle Research and Cell Motility* **18**, 161–167.

Fulceri, R., Bellomo, G., Gamberucci, A., Romani, A. & Benedetti, A. (1993). Physiological concentrations of inorganic phosphate affect MgATP-dependent Ca^{2+} storage and inositol trisphosphate-induced Ca^{2+} efflux in microsomal vesicles from non-hepatic cells. *Biochemical Journal* **289**, 299–306.

Godt, R. E. & Maughan, D. W. (1988). On the composition of the cytosol of relaxed skeletal muscle of the frog. *American Journal of Physiology* **23**, C591–604.

Godt, R. E. & Nosek, T. M. (1989). Changes of intracellular milieu with fatigue or hypoxia depress contraction of skinned rabbit skeletal and cardiac muscle. *Journal of Physiology* **412**, 155–180.

Goldman, D. E. (1943). Potential, impedance and rectification in membranes. *Journal of General Physiology* **27**, 37–60.

Guse, A. H., Silva, C. P., Weber, K., Ashamu, G. A., Potter, B. V. & Mayr, G. W. (1996). Regulation of cADP-ribose-induced Ca^{2+} release by Mg^{2+} and inorganic phosphate. *Journal of Biological Chemistry* **271**, 23946–23953.

Kabbara, A. A. & Allen, D. G. (1999). The role of calcium stores in fatigue of isolated single muscle fibres from the cane toad. *Journal of Physiology* **519**, 169–176.

Kourie, J. I. (1997*a*). A redox O_2 sensor modulates the SR Ca^{2+} countercurrent through voltage- and Ca^{2+}-dependent Cl^- channels. *American Journal of Physiology* **272**, C324–332

Kourie, J. I. (1997*b*). ATP-sensitive voltage- and calcium-dependent chloride channels in sarcoplasmic reticulum vesicles from rabbit skeletal muscle. *Journal of Membrane Biology* **157**, 39–51.

Kourie, J. I. (1999). pH-modulation of chloride channels from the sarcoplasmic reticulum of skeletal muscle. *Journal of Membrane Biology* **167**, 73–83.

Kourie, J. I., Foster, P. S. & Dulhunty, A. F. (1997). Inositol polyphosphates modify the kinetics of a small chloride channel in skeletal muscle sarcoplasmic reticulum. *Journal of Membrane Biology* **157**, 147–158.

Kourie, J. I., Laver, D. R., Ahern, G. P. & Dulhunty, A. F. (1996*a*). A calcium-activated chloride channel in sarcoplasmic reticulum vesicles from rabbit skeletal muscle. *American Journal of Physiology* **270**, C1675–1686.

Kourie, J. I., Laver, D. R., Junankar, P. R., Gage, P. W. & Dulhunty, A. F. (1996*b*). Characteristics of two types of chloride channel in sarcoplasmic reticulum vesicles from rabbit skeletal muscle. *Biophysical Journal* **70**, 202–221.

Laver, D. R. & Curtis, B. A. (1996). Surface potentials measure ion concentrations near lipid bilayers during rapid solution changes. *Biophysical Journal* **71**, 722–731.

Laver, D. R., Roden, L. D., Ahern, G. P., Eager, K. R., Junankar, P. R. & Dulhunty, A. F. (1995). Cytoplasmic Ca^{2+} inhibits the ryanodine receptor from cardiac muscle. *Journal of Membrane Biology* **147**, 7–22.

Margolis, M. J. (1966). *Chemical Principles in Calculation of Ionic Equilibria.* Macmillan, New York.

Marks, P. W. & Maxfield F. R. (1991). Preparation of solutions with free calcium concentration in the nanomolar range using 1,2-bis(o-aminophenoxy)ethane-N,N,N′,N′-tetraacetic acid. *Annals of Biochemistry* **193**, 61–71.

Mezna, M. & Michelangeli, F. (1998). The role of inorganic phosphate in regulating the kinetics of inositol 1,4,5-trisphosphate-induced Ca^{2+} release: a putative role for endoplasmic reticulum phosphate transporters. *Biochimica et Biophysica Acta* **1373**, 270–276.

Nordeen, M. H., Jones, S. M., Howell, K. E. & Caldwell, J. H. (2000). GOLAC: An endogenous anion channel of the golgi species. *Biophysical Journal* **78**, 2918–2928.

Oba, T., Koshita, M. & Van Helden, D. F. (1996). Modulation of frog skeletal muscle ryanodine receptor/Ca^{2+} release channel gating by anion channel blockers. *American Journal of Physiology* **271**, C819–824.

Posterino, G. S. & Fryer, M. W. (1998). Mechanisms underlying phosphate-induced failure of Ca^{2+} release in single skinned skeletal muscle fibres of the rat. *Journal of Physiology* **512**, 97–108.

Saito, A., Seiler, S., Chu, A. & Fleischer, S. (1984). Preparation and morphology of sarcoplasmic reticulum terminal cisternae from rabbit skeletal muscle. *Journal of Cellular Biology* **99**, 875–885.

Sitsapesan, R. (1999). Similarities in the effects of DIDS, DBDS and suramin on cardiac ryanodine receptor function. *Journal of Membrane Biology* **168**,159–168.

Smith, J. S., Coronado, R. & Meissner, G. (1986). Single-channel calcium and barium currents of large and small conductance from sarcoplasmic reticulum. *Biophysical Journal* **50**, 921–928.

Smith, R. M. & Alberty, R. A. (1956). The apparent stability constants of ionic specieses of various adenosine phosphates with monovalent cations. *Journal of Physics and Chemistry* **60**, 180–184.

Somlyo, A. V., Gonzalez-Serratos, H., Shuman, H., MacLellan, G. & Somlyo, A. P. (1981). Calcium release and ionic changes in the sarcoplasmic reticulum of tetanized muscle: An electron-probe study. *Journal of Cell Physiology* **90**, 577–594.

Stefanova, H. I., Jane, S. D., East, J. M. & Lee, A. G. (1991*a*). Effects of Mg^{2+} and ATP on the phosphate transporter of sarcoplasmic reticulum. *Biochimica et Biophysica Acta* **1064**, 329–34

Stefanova, H. I., East, J. M. & Lee, A. G. (1991*b*). Covalent and non-covalent inhibitors of the phosphate transporter of sarcoplasmic reticulum. *Biochimica et Biophysica Acta* **1064**, 321–328.

Tanifuji, M., Sokabe, M. & Kasai, M. (1987). An anion channel of sarcoplasmic reticulum incorporated into planar lipid bilayers: single-channel behaviour and conductance properties. *Journal of Membrane Biology* **99**, 103–111.

Acknowledgements

Our thanks to Suzy Pace and Joan Stivala for preparing SR vesicles and to Drs Martin Fryer and Graham Lamb for their helpful suggestions. Dr Derek Laver was supported by a grant from the National Health & Medical Research Council of Australia (no. 9836486) and Gerlinde Lenz was supported by a grant from the Australian Research Council (ARC small grant).

Corresponding author

D. R. Laver: School of Biochemistry and Molecular Biology, Faculty of Science, Australian National University, Canberra, ACT 0200, Australia.

Email: derek.laver@anu.edu.a